Sedimentary sequences offshore northeastern Taiwan and the offshore projection of the Shanjiao Fault zone

Quang-Minh Nguyen [a,b], Shu-Kun Hsu [a,c,*], Andrew Tien-Shun Lin [a], Chih-Cheng Yang [d]

[a] *Department of Earth Sciences, National Central University, Taiwan*
[b] *Institute of Marine Geology and Geophysics, Vietnam Academy of Science and Technology, Hanoi, Viet Nam*
[c] *Institute of Earth Sciences, Academia Sinica, Taipei 11529, Taiwan*
[d] *Exploration and Production Business Division, CPC Corporation, Taiwan*

A B S T R A C T

The offshore area of northern Taiwan is currently in an extensional regime, known for a post-collision area of the Taiwan mountain belt that has formed due to the oblique collision of the Philippine Sea Plate against the Eurasian continental margin since the late Miocene. The active collision has undergone a progressive migration of the Taiwan mountain belt from the northeast to the southwest direction. After the relaxation of the compressional stress due to the westward subduction of the Philippine Sea Plate, the northern Taiwan orogen has collapsed together with the opening of the southern Okinawa Trough. Here, we show the transitional process from compressional to extensional regime in the area off northern Taiwan and reconstruct the tectono-sedimentary evolution by using multi-channel reflection seismic data. We process and interpret multi-channel seismic profiles and use borehole data to determine the ages of sedimentary units and stratal surfaces/unconformities. Based on the seismic facies, we have recognized two distinctive domains separated by the Offshore Shanjiao Fault (OSF): a shelf basin to the northwest and a collapsed zone to the southeast. The tectono-sedimentary evolution off northern Taiwan since the late Miocene can be described in 4 stages. (1) The compressional structures off northern Taiwan were formed during the collision period starting around 6 Ma, a series of folds-and-thrusts aligned in the NE-SW direction. (2) Due to the oblique collision, some NW-SE-trending strike-slip faults were developed across the collision belt to accommodate the differential displacements between two adjacent segments of the folded belt. (3) During the transition from compressional to extensional regime at about 2.7 Ma, a post-collisional erosion and subsidence occurred in the collapsed zone to form the basal unconformity. This post-collisional collapse is associated with the opening of the southern Okinawa Trough, a back-arc basin, due to the westward migration of the Philippine Sea Plate subduction beneath the southern Ryukyu arc. (4) The offshore area of northern Taiwan has subsided continuously with sediment accumulation since the early Pleistocene (~2.0 Ma), accompanying the rifting of the southern Okinawa Trough.

1. Introduction

Taiwan mountain belt is known as a result of the oblique arc-continent collision between the Luzon arc of the Philippine Sea plate and the Eurasian continental margin since the late Miocene (e.g. Teng, 1990; Sibuet and Hsu, 2004). Due to the oblique collision, the Taiwan orogen has been interpreted to migrate in a southwestward direction (Suppe, 1984; Teng, 1996; Sibuet and Hsu, 2004). The Taiwan mountain belt has evolved through time and its tectonic regime can be described from north to south as the following stages: the post-collisional area in offshore northern Taiwan and this tectonic regime is linked to the back-

arc opening of the southern Okinawa Through; collisional Taiwan orogen; and the pre-collisional area in the northernmost Manila subduction zone off southern Taiwan (Teng et al., 2000, Teng and Lin, 2004; Malavieille et al., 2002; Sibuet and Hsu, 2004). There are several models to explain the formation of Taiwan orogen as well as the early stage of collision in the offshore area of northern Taiwan, such as the migrating arc-continent collision (Suppe, 1984; Sibuet and Hsu, 2004), the flipping of subduction polarity and resulting extensional tectonics in northern Taiwan (Teng, 1996, Teng et al., 2000; Chang et al., 2017), the collision and opening of the southern Okinawa Trough (Hsu and Sibuet, 1995, Hsu et al., 1996; Sibuet et al., 1995, 1998; Kong et al., 2000), or a

simultaneous mountain building for the Taiwan orogenic belt (Lee et al., 2015).

Although most of the Taiwan island is still under a compressive regime, the northernmost of Taiwan and its offshore area has undergone continental rifting due to the inversion of tectonic stress from compression to extension (Suppe, 1984; Teng, 1996; Hsu and Sibuet, 1995; Sibuet and Hsu, 2004; Chang et al., 2017). In consequence, some of the NE-SW-trending thrust faults formed during the compressional stage may have inverted as normal faults (Hsiao et al., 1998; Sibuet et al., 1998; Tsai et al., 2018). The normal faulting has caused the development of a series of half-grabens filled with Quaternary sediments (Kong et al., 2000). Although the extensional tectonism in northern offshore Taiwan is generally agreed, a holistic understanding of its geological evolution is lacking. We interpret multi-channel seismic data and well-log data to reconstruct the tectonic history from compressive to extensional stages of the area off northern Taiwan.

2. Geological background

Taiwan island is located in the transition zone where the northwesterly moving Philippine Sea Plate is subducting beneath the Eurasian Plate beneath the Ryukyu arc-trench system but it overrides the Eurasian Plate along the Luzon arc-trench system in the south (Fig. 1) (Hall, 2002; Seno et al., 1993, Sibuet and Hsu, 2004). Due to this northwesterly plate motion, the northern tip of the Luzon arc started to collide with the Eurasian margin at ~9 Ma, creating the northern Taiwan mountain belt (Sibuet et al., 2002). The initial collision point of the Luzon arc against the Eurasian margin could be at about 400–500 km off NE of Taiwan (Teng, 1990; Hsiao et al., 1998; Sibuet and Hsu, 2004). With the present-

day convergence rate (8 cm/year, Yu et al., 1997) as a reference, the initial collision may start at 9 Ma or 6 Ma, assuming the rate of plate convergence of 5.6 cm/year or 7.1 cm/year, respectively (Sibuet and Hsu, 2004).

The East China Sea shelf basin is the largest Cenozoic sedimentary basin of the continental margin to the east China (Fig. 1) (Zhou et al., 1989). It is divided into a series of sub-basins, separated by basement highs or paleo-uplifts (Hsu et al., 2001). In the southern part of the East China Sea shelf basin, several Paleogene sub-basins bounded by NE-SW-trending normal faults are filled with *syn*-rift sediments and draped by Neogene post-rift strata (Sun, 1985; Wang et al., 2019). The offshore area of northern Taiwan was a part of the East China Sea shelf basin before the collision in the late Miocene (Teng, 1990; Kong et al., 2000; Wang et al., 2019). The rifted-margin strata were strongly folded-and-thrusted to become a mountain belt during the collision (Kong et al., 2000). After the inversion of compressive to extensional stresses, the area has undergone extension, linked to the development of the rifted southern Okinawa Trough (Teng, 1996).

Located in the area between the Kyushu and Taiwan islands, the Okinawa Trough is an active back-arc basin (Sibuet et al., 1998; Tsai et al., 2021) (Fig. 1). Its early rifting phase was dated as late Miocene in the northern Okinawa Trough while the southern Okinawa Trough started to open in the Pleistocene (Letouzey and Kimura, 1985; Kimura, 1985; Sibuet et al., 1998). In the southern Okinawa Trough, the initial phase of the opening corresponds to the reactivation of the NE-SW-trending thrust fault system which was previously formed during the collision of the Luzon arc against the Eurasian margin, as suggested by previous studies (e.g. Hsiao et al., 1998; Sibuet et al., 1998). Some volcanic rocks thus intruded along the active NE-SW-trending normal faults during the Pleistocene (Sibuet et al., 1998; Wang et al., 2004).

In addition to the NE-SW-trending fault systems, there are some NW-SE-trending morphological features such as the Keelung Valley, Mienhua Canyon and North Mienhua Canyon which are obvious on the bathymetric map (Fig. 1). Based on bathymetric lineaments and reflection seismic data, Song et al. (2000) suggested that the Keelung Valley is situated at a set of right-lateral strike-slip faults. Other NW-SE-trending strike-slip faults are also interpreted from data sets of bathymetry, magnetic and gravity anomalies, earthquakes, and reflection seismic by Hsu et al. (1996) and Kong et al. (2000). The NW-SE-trending strike-slip faults probably developed during the collision between the northern tip of the Luzon arc and the Eurasian continental margin (Hsu et al., 1996).

3. Multi-channel seismic data processing and borehole data

The data used in this study include 68 lines of 2D multi-channel seismic (MCS) profiles which have a total length of about 100 km long (Fig. 2). The MCS data were collected during the surveys from 2006 to 2019. The acquisition configurations are not always the same due to the different purposes of the cruises, especially the streamer lengths. In total, there are 18 profiles collected with a long streamer (about 1500 m long) in 2013 and 2019, but the rest cruises used a short streamer (about 180 m long). The reflection seismic data constitutes a good data coverage in our study area.

We have processed all the 68 MCS profiles using ProMAX, Landmark Graphics Corporation, then included them in our analysis and results. A brief description of the processing steps is as follows. Firstly, the bad shots and excessively noisy channels were removed. A predictive deconvolution was performed to compress the source wavelet and a band-pass filter was applied to reduce the low-and high-frequency noise signals boosted after deconvolution. The data were sorted into the common mid-point domain (CMP) by assuming the straight-line geometry of the streamer; CMP spacings of 12.5 m and 6.25 m, respectively, were defined for the long and short streamers. Velocity analysis was performed on selected groups of CMP gathers and spatially interpolated to apply a normal-move-out correction. True amplitude recovery was used to enhance the amplitude data at depth and to effectively improve

Fig. 1. Tectonic and topographic/bathymetric map of Taiwan and adjacent areas. In northern Taiwan and its offshore area, fault behavior changes gradually from thrust faults in the south to normal faults in the north. The deformation front, Manila Trench and Ryukyu Trench are inferred from previous studies (Sibuet and Hsu, 2004; Yu, 2005; Lin et al., 2008; Hsu et al., 2013). The convergence rate (8 cm/yr) is proposed by Yu et al. (1997). The red dashed lines indicate faults or trenches. The blue rectangle indicates our study area. NMHC: North Mienhua Canyon, MHC: Mienhua Canyon, and KLV: Keelung Valley. (For interpretation of the references to colour in this figure legend, the reader is referred to the web version of this article.)
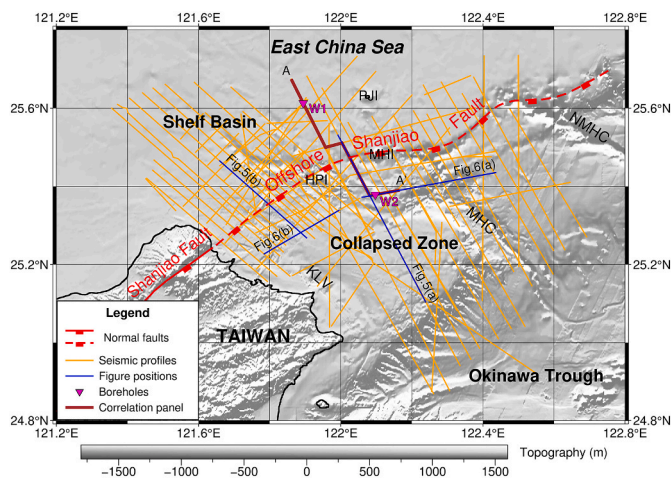
Fig. 2. A topographic/bathymetric map with locations of the seismic profiles and borehole data were used in this study. The MCS data were acquired by several research cruises onboard R/V Ocean Researcher 1, R/V Ocean Researcher 2 and R/V Legend from 2006 to 2019. Borehole data of W1 and W2 are from well reports of Blackie et al. (1975) and Yang et al. (1985), respectively. A-A' is the position of Fig. 4. NMHC: North Mienhua Canyon, MHC: Mienhua Canyon, KLV: Keelung Valley, HPI: Huaping islet, MHI: Mienhua islet, PJI: Pengjia islet.

the quality of the MCS images, especially for the deeper sections. The data were stacked to enhance the true stratal signal and reduce the random noise. Finally, the data were migrated by using the most satisfactory root mean square velocities and interpreted in the time domain. Only the top 3 s two-way travel time (TWT) of the MCS data are shown in seismic profiles because no clear coherent reflections are recognized below 3 s TWT. Additionally, stratigraphic information and well-logs are obtained from W1 and W2 boreholes (Blackie et al., 1975; Yang et al., 1985) (Fig. 2). The depth domain of well-log data is converted into the time domain using borehole check-shot information and the drilled borehole stratigraphy is tied to seismic profiles.

4. Results

Based on the principles of seismic stratigraphic interpretation (e.g. Vail and Mitchum, 1977; Mitchum et al., 1997), well-log and seismic reflection data are used to identify seismic facies and seismic units in our study area. We define four stratigraphic units and four unit-boundaries with references to previous studies (Blackie et al., 1975; Yang et al., 1985; Hsiao et al., 1998; Kong et al., 2000; Chang et al., 2017) (Fig. 3).

We focus on the Miocene and younger units because we aim to reconstruct the evolution model in the offshore area of northern Taiwan since the late Miocene.

4.1. Seismic to borehole correlation

There are two deep boreholes, W1 and W2, available for this study (Fig. 4). The wireline logs from boreholes W1 and W2 are converted into time domain by using sonic logs from respective wells in order to carry out borehole-to-seismic correlation. The results are shown in Fig. 4, where for each well, the gamma ray log (GR) is shown at the left and the sonic log (DT) and resistivity log (ILD) are shown at the right.

Located in the East China shelf basin, well W1 has a total depth of 4029 m (Blackie et al., 1975) (Figs. 2 and 4). The drilled stratigraphy from bottom to top is as follows (Blackie et al., 1975): (1) *syn*-rift strata spanning from Paleogene to Eocene (~NP9-NP16, below 2076 m), (2) post-rift strata with ages ranging from late Oligocene to Pleistocene (above 2076 m to the seafloor). The above two stratigraphic packages are separated by the post-rift unconformity at 2076 m. The post-rift strata are further divided into late Oligocene to Miocene Series (2076–745 m), Pliocene Series (745–620 m), and Pleistocene Series (620 m to the seafloor) according to Blackie et al. (1975). Seismic profile across W1 well shows that parallel or semi-parallel strata overlying the post-rift unconformity (PRU) (Fig. 4), implying that the sediments were gradually accumulated from Oligocene to Quaternary without major faulting. It suggests that the area was not incorporated in the orogenic processes during the collision of the Luzon arc with the Eurasian margin in the late Miocene. The PRU, separated the underlying Paleogene *syn*-rift and the overlying Oligocene to Quaternary post-rift sediments, is dated as probably late Eocene to early Oligocene in age (Blackie et al., 1975, SP ~350, Fig. 4).

Located in the area between the continental shelf and continental slope of the East China Sea, well W2 reaches a depth of about 3492 m (Yang et al., 1985) (Figs. 2 and 4). An angular unconformity, named as the basal unconformity (BU) at about 1.2 s TWT at W2 borehole is observed (SP ~1850, Fig. 4). The drilled stratigraphy from bottom to top as reported in Yang et al. (1985) is as follows: (1) Miocene Series (3492–1152 m), (2) Pleistocene Series (1152 m to the seafloor). The above two stratigraphic packages are separated by an angular unconformity (BU) as reported in Yang et al. (1985) and seen from reflection seismic profiles as shown in Fig. 4.

In the southeastern part of the seismic profile (SP 1300–2300, Fig. 4), the tilted and folded strata beneath the BU is of Miocene in age, suggesting that this area was a part of fold-and-thrust belts during the collision. The Pleistocene sediment overlies directly on top of BU and a lack of Pliocene strata indicates that the collision process may continue until the Pliocene.

Epoch	Age (Ma)	Unit		Unit boundary		Tectonic event
		ShB	CoZ	ShB	CoZ	
Quaternary (F)	0	Fa	Fb		BU	- Rifting and volcanic activities, opening of the southern OT
	2.6			R6		
Pliocene (E)		Ea		OSF		- Collision of the Luzon arc with the Eurasian continent
	5.3			R5		
Miocene - Oligocene? (D)		Da	Db			- Opening of the central-north OT - Subduction of the PSP under the RA in the northern part
	33.9			PRU		
Eocene (C)		Ca				- Continental rifting

Fig. 3. Seismic units and tectonic events in the offshore area of northern Taiwan. Wavy lines indicate unconformity and diagonal lines indicate missing strata. PRU: Post-Rift Unconformity, BU: Basal Unconformity, R5: Miocene-Pliocene boundary, R6: Pliocene-Quaternary boundary, CoZ: Collapsed Zone, ShB: Shelf Basin, OSF: Offshore Shanjiao Fault, OT: Okinawa Trough, PSP: Philippine Sea Plate, RA: Ryukyu Arc.
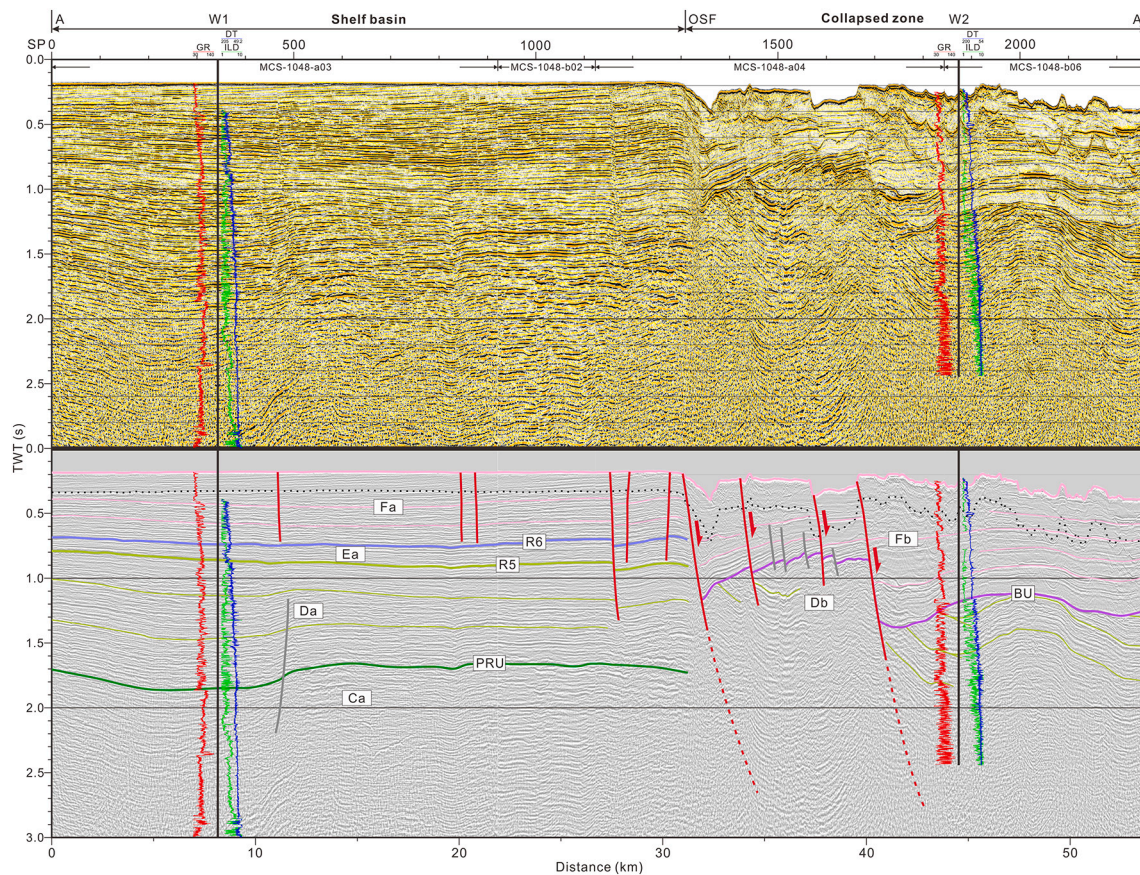
Fig. 4. Seismic to well correlation showing the seismic units, age and major stratal surfaces in the offshore area of northern Taiwan. Wells W1 and W2 are adapted from Blackie et al. (1975) and Yang et al. (1985), respectively. GR: Gamma-ray, DT: Sonic log, ILD: Induction resistivity, SP: Shot point, TWT: Two-way travel time, OSF: Offshore Shanjiao Fault. Refer to Fig. 3 for symbols of seismic units and Fig. 2 for profiles and well locations.

4.2. Multi-channel seismic data interpretation

The seismic profiles show that normal faults are the predominant structures, particularly in the southeast corner of our study area (herein referred as the collapsed zone) (Figs. 4 to 6). Along the NW-SE-oriented seismic profiles, MCS-1048-a04 and MCS-960-e05 (Fig. 5), the development of NE-SW-trending and tilted block faulting suggest that the collapsed zone is under extension. The western boundary of the collapsed zone is defined by a normal fault with large offset (SP ~ 350 in Fig. 5a and SP ~800 in Fig. 5b) that delimits the semi-parallel seismic configurations of the Oligocene-Miocene strata (Da) in the shelf basin from those oblique or folded strata (Db) in the collapsed zone. Based on the NW-SE-oriented seismic data (e.g. Figs. 4 and 5) and the different stratal configurations on both sides of this large offset fault, we connect the offshore segments of this fault and consider it as the Offshore Shanjiao Fault (OSF) (Fig. 2). On the seismic profile, MCS-960-e05 (SP 500–1000, Fig. 5b), when comparing the top boundary of Unit D on both sides of the OSF, the strata surface (R5) on the footwall is deeper than the BU surface on the hanging wall. It implies that the OSF was a thrust fault during the collision process, and then it has been reactivated as a normal fault during the later extensional stage.

Besides, the bathymetric data have been used as a reference for tracking the strike of active faults. Based on the integrated analysis, the normal faults align mostly in the NE-SW direction in the collapsed zone. There are, however, some faults trending in NW-SE directions developed as seen from seismic data (Fig. 6). These NW-SE-trending fault systems occur mostly beneath submarine channels such as the Keelung Valley and the Mienhua Canyon. Along the NE-SW-oriented seismic profile MCS-1048-b05 (SP 200–400, Fig. 6b), there is a NW-SE trending normal fault along the Keelung Valley. This normal fault links to an old positive

flower structure in the seismic profile from 0.7 to 2.0 s TWT. It may indicate that an NW-SE-trending strike-slip fault was formed by transpressional stress in the late Miocene. In the MCS-1048-b06 (SP 700–1300, Fig. 6b), an array of NW-SE-trending normal faults also exist beneath the Mienhua Canyon.

On the seismic profile, MCS-1048-a04 (SP 900–1100, Fig. 5a), the BU has obscured due to seafloor multiples and no clear stratal reflections appear on the seismic image. We suggest that this is due to indurated rocks near the seafloor, possibly volcanic rocks, similar to the observation near the submarine volcanoes in profile MCS-960-e5 (SP 650–800, Fig. 5b) or the volcanic Mienhua and Pengjia islets (Chang et al., 2021). The magmatic activities might have occurred since the early Pleistocene as suggested by regional magmatic activities (Wang et al., 2004).

4.3. Seismic units

Seismic Unit C is the *syn*-rift sediments deposited in the eastern part of the shelf basin during the Eocene (Blackie et al., 1975). The seismic facies shows reflections of semi-continuous and moderate amplitude. The Paleogene syn-rift sediments were interpreted as deltaic to marginal-marine sediments (Wang et al., 2019).

Seismic Unit D is possibly of Oligocene–Miocene in age with reflections exhibiting semi-continuous and moderate amplitude. The isopach of Unit D in the shelf basin (Da) is almost uniform in thickness, around 800–1000 ms TWT (Fig. 7a), suggesting stable tectonics of the area during sediment accumulation of this seismic Unit. Nevertheless, the reflection configurations of Unit D across the OSF changes abruptly from semi-parallel pattern in the shelf basin (Da) to tilted and/or folded pattern in the collapsed zone (Db) (Fig. 5). The existence of Unit Db implies that the collapsed zone is part of the East China shelf basin
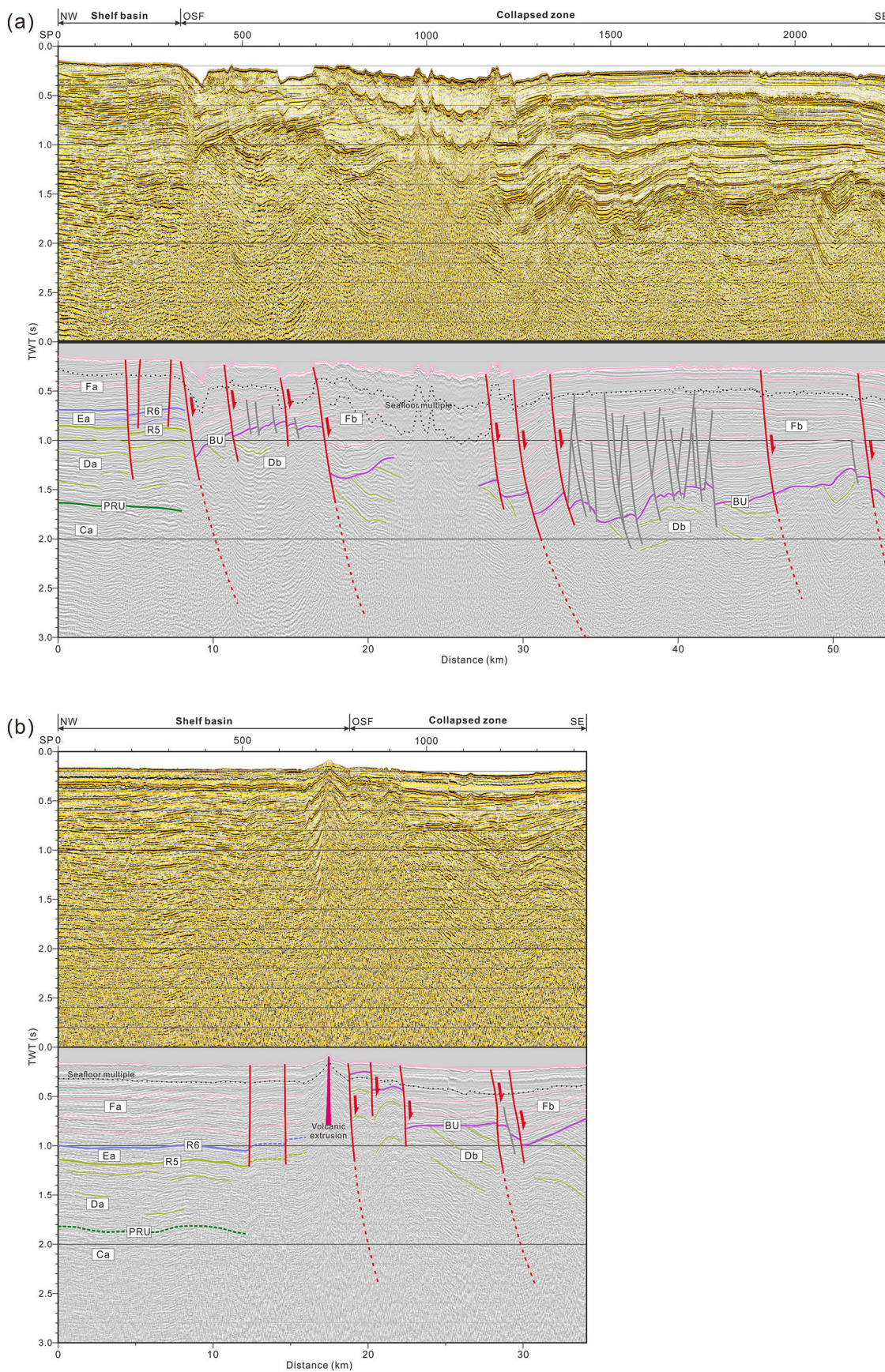
Fig. 5. NW-SE-oriented multi-channel seismic profiles MCS-1048-a04 (a) and MCS-960-e05 (b) and their corresponding interpretations. These two profiles run from the shelf basin to the collapsed zone and perpendicular to the Offshore Shanjiao Fault. SP: Shot point, TWT: Two-way travel time, OSF: Offshore Shanjiao Fault. Refer to Fig. 3 for symbols of seismic units and Fig. 2 for locations.
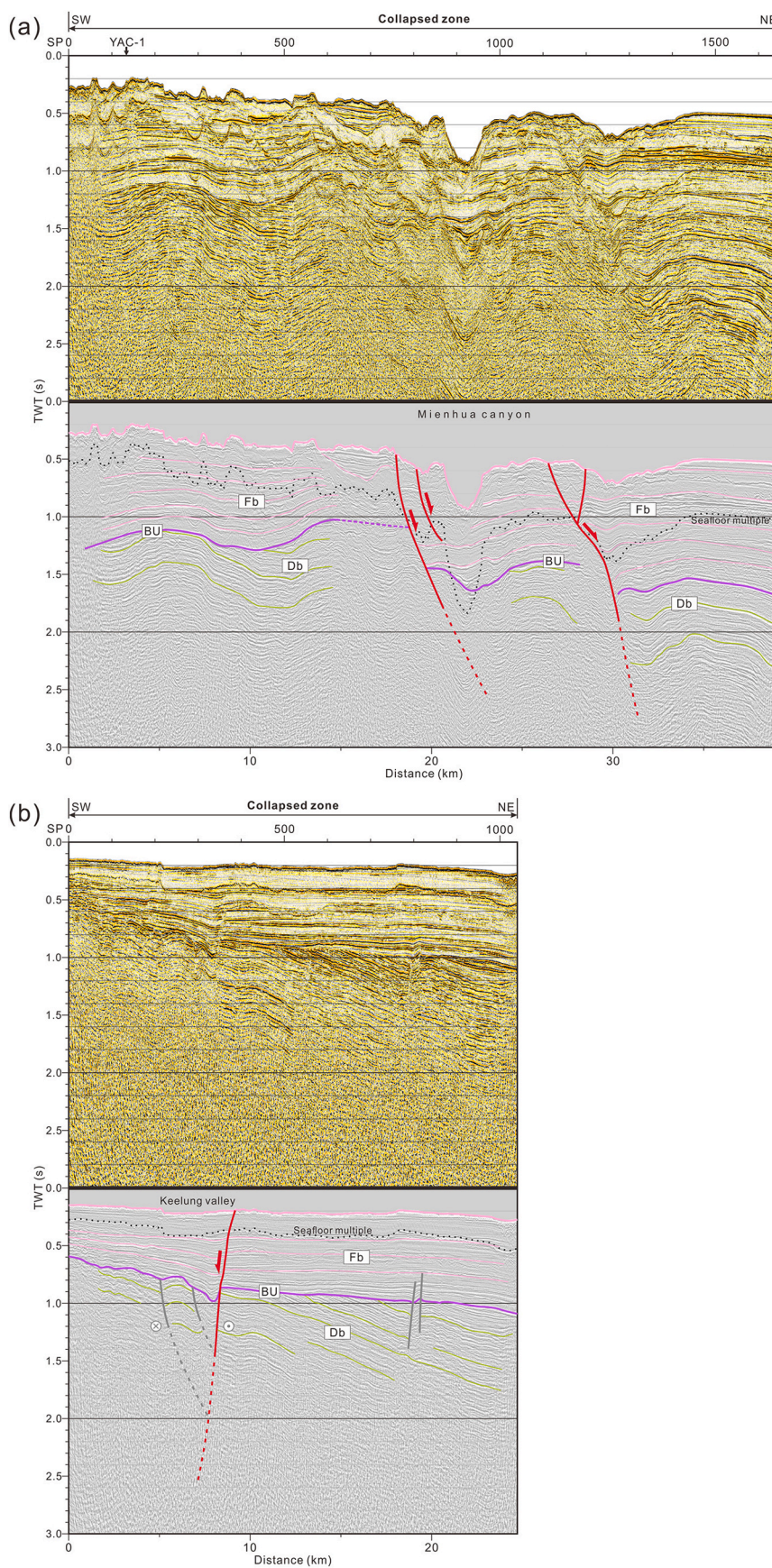
Fig. 6. NE-SW-oriented multi-channel seismic profiles MCS-1048-b06 (a) and MCS-1048-b05 (b) and their interpretations. These two profiles run along the eastern side of the Offshore Shanjiao Fault. SP: Shot point, TWT: Two-way travel time, OSF: Offshore Shanjiao Fault. Refer to Fig. 3 for symbols of seismic units and Fig. 2 for locations.
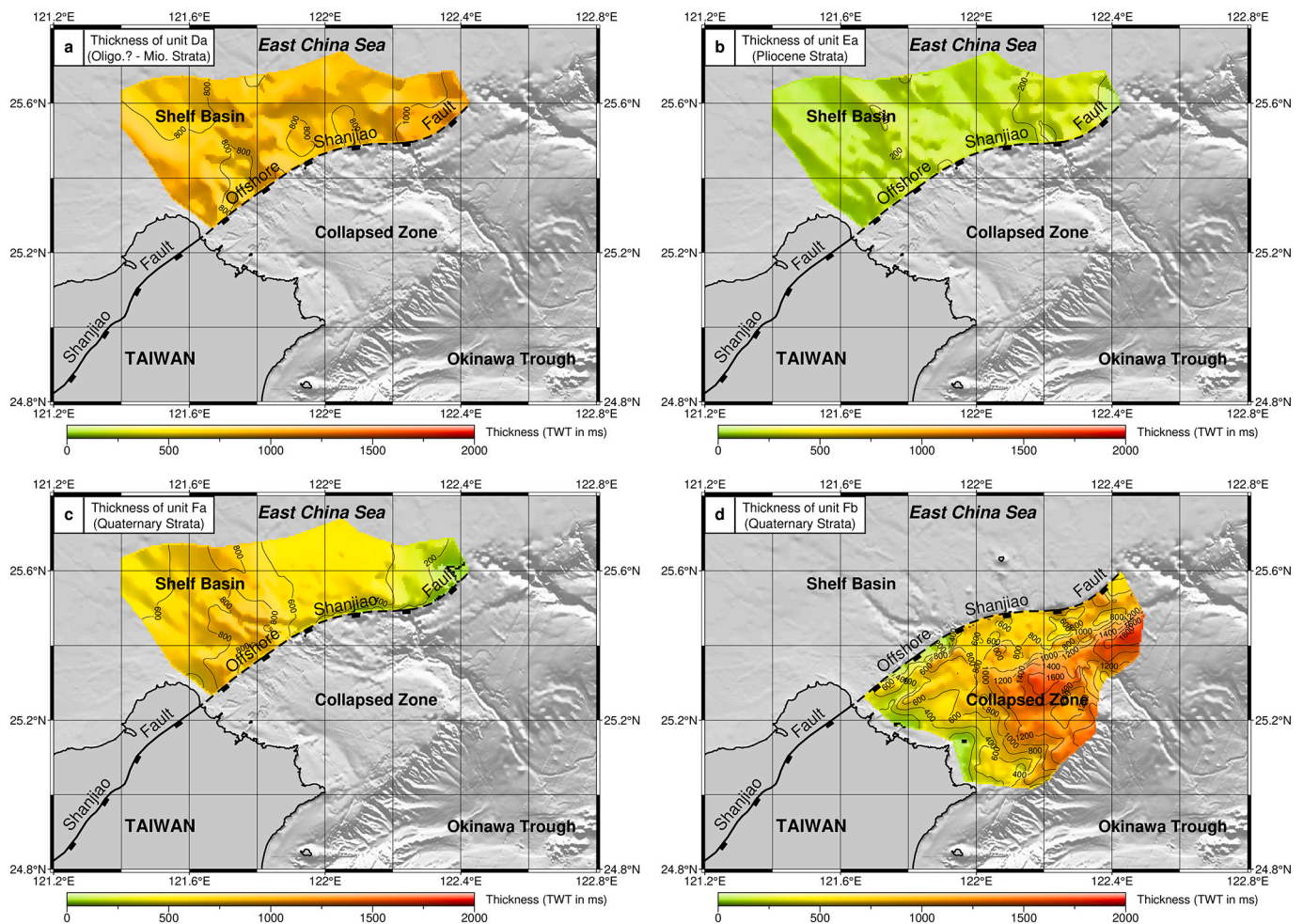
Fig. 7. Sediment isopach contour maps of Units D to F in millisecond TWT. (a) Thickness of Unit Da (Oligocene?-Miocene strata). (b) Thickness of Unit Ea (Pliocene strata). (c) Thickness of Unit Fa (Quaternary strata in the shelf basin). (d) Thickness of Unit Fb (Quaternary strata in the collapsed zone). The contour interval is 200 ms TWT.

before the collision. Therefore, we suggest that the OSF was the thrust front of the Taiwan mountain belt in the late Miocene. The PRU separates the underlying Unit C and its overlying Unit D (Fig. 8a). However, PRU could not be identified in the collapsed zone due to the intensively folded strata and ambiguous reflection signals.

Seismic Unit E is of Pliocene in age. It shows seismic reflection with semi-continuous and low to moderate amplitude. Sediment isopach of this unit exhibits a thin layer (i.e., less than 300 ms TWT) and only occurs in the shelf basin (Ea) (Fig. 7b). The Unit Ea is separated from Unit Da by unit boundary R5 (Fig. 8b).

Seismic Unit F is of Quaternary in age. It shows continuous and high amplitude seismic reflections in the shelf basin (Fa), and semi-continuous and moderate to high amplitude reflections in the collapsed zone (Fb), respectively. In the shelf basin, Unit Fa shows parallel strata with thickness up to 900 ms TWT (Fig. 7c) and it is separated from the underlying Unit Ea by unit boundary R6 (Fig. 8c). In the collapsed zone, the thickness of Unit Fb is controlled by tilted fault-blocks and shows a wedge shape of westward divergent strata (SP 350–900 and 1200–2200, Fig. 5a). It shows that Unit Fb consists of grabens or half-grabens-infilled sediments due to normal faulting. The Unit Fb is floored by an angular basal unconformity, BU (Fig. 8d). The BU surface shallows gradually from the NE to SW, indicating that the extensional regime has propagated from NE to SW in the offshore area of northern Taiwan.

5. Discussion

5.1. The OSF and features of faults off northern Taiwan

The characteristics of the faults in the offshore area of northern Taiwan were discussed in previous studies (e.g., Hsiao et al., 1998; Song et al., 2000). The NE-SW-trending faults were identified by using seismic imaging and bathymetric data. Based on our multi-channel seismic data (e.g., Figs. 4 and 5), we connect the NE-SW-trending OSF to the onshore Shanjiao Fault by using the stratigraphic correlation on both sides of the fault. The OSF is considered as the thrust front during the former collision stage in the study area and it has become a large-offset normal fault during crustal extension. Therefore, the projection of the OSF provides a good constraint on constructing the tectonic evolution model off northern Taiwan. In the collapsed zone, a series of NE-SW-trending normal faults with large offsets can be seen on the seismic profiles (Figs. 4 and 5). We suggest that these large-offset normal faults are reactivated along pre-existing thrust faults. Although the reactivation of NE-SW-trending faults was mentioned by Hsiao et al. (1998), Sibuet et al. (1998) and Tsai et al. (2018), the obvious evidence of the reactivation of OSF and its projection is firstly proposed base on our new seismic interpretation (Fig. 5) and distribution map of the seismic units (Figs. 7 and 8).

The oblique collision between the northern tip of the Luzon arc and the Eurasian plate produced a curved collisional belt off northern Taiwan (Sibuet and Hsu, 2004). Within the curved thrust belt, the NE-
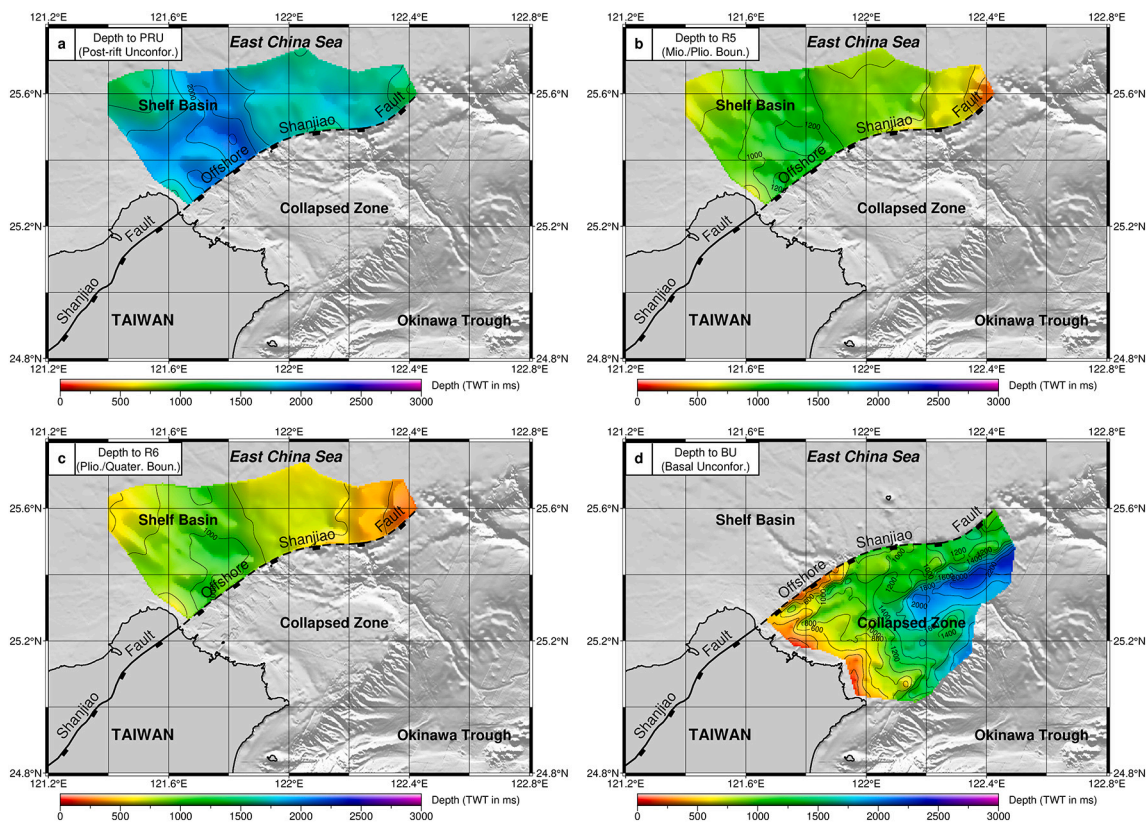
Fig. 8. Time contour maps of the depths to the unit boundaries (unit: millisecond). (a) Depth to PRU (Post-Rift Unconformity). (b) Depth to R5 (Miocene-Pliocene boundary). (c) Depth to R6 (Pliocene-Quaternary boundary). (d) Depth to BU (Basal Unconformity). The contour interval is 200 ms TWT.

SW-trending thrusts could be separated by some NW-SE-trending strike-slip faults due to differential compressional stresses on the reverse faults as observed in other examples (e.g., Twiss and Moores, 1992). Song et al. (2000) indicated a flower structure beneath the Keelung Valley, which implies that the NW-SE-trending strike-slip fault was formed by transpressional stresses (SP 200–400, Fig. 6b). After the relaxation of compressional stress, a few branches of strike-slip faults continue to develop as normal faults which are found beneath the Mienhua Canyon (SP 700–1300, Fig. 6a) and Keelung Valley (SP 300–400, Fig. 6b). Those NW-SE-trending faults have separated several segments of the extensional structures during the Quaternary. The development of the NW-SE-trending Keelung Valley and Mienhua Canyon was possibly influenced by the existence of the strike-slip faults. Therefore, the locations of the submarine channels off northern Taiwan might provide a constraint on the geometry of NW-SE-trending strike-slip faults during compression period.

5.2. Reconstruction of the tectonic evolution off northern Taiwan

In this study, we follow the model of Sibuet and Hsu (2004) to discuss the tectonic development in the offshore area of northern Taiwan (Figs. 9 and 10). They proposed that the collision started at ~9 Ma farther to the NE of the study area, assuming a constant convergence rate of 5.6 cm/yr between the Eurasian Plate and the Philippine Sea Plate. We thus suggest that the study area may start to experience compression at ~6 Ma due to the southwestward migration of collision.

5.2.1. Reconstruction at 6 Ma

Before 6 Ma, the offshore area of northern Taiwan was a rifted Eurasian continental margin (Teng, 1990; Kong et al., 2000; Wang et al., 2019), where Units C and D appeared as semi-parallel configurations. At 6 Ma, the northern tip of the Luzon arc collided with the Eurasian continental margin off northern Taiwan, forming the proto-Taiwan

mountain belt (Sibuet and Hsu, 2004). As a result of the compressional stress, Units C and D were folded, becoming thrust sheets (Unit Db). A series of thrust faults were also formed within the thrust sheets during the period. Among the thrusts, the OSF is the northwestern-most thrust fault and is known as the thrust front of the proto-Taiwan mountain belt.

5.2.2. Reconstruction at 4 Ma

To the southeast portion of OSF, the Eurasian continental margin continued to be shortened and thickened by the converging Philippine Sea plate (Teng, 1996). Unit Db and its underlying strata were folded-and-thrusted to form the proto-Taiwan thrust belts in the study area (Sibuet and Hsu, 2004). Whereas, to the northwest of OSF, Unit Ea was accumulated in the foreland basin and in front of the deforming and uplifting compressional belt. Due to the oblique collision process (Teng, 1996; Sibuet and Hsu, 2004), the compressional stress gradually migrated from the NE to SW direction, leading to various segments of thrusted faults. In consequence, NW-SE-trending dextral strike-slip faults were formed to accommodate the differential stresses on both sides of the belt segments. The pre-existing thrust faults could have been cut into fault segments and display offsets along the NW-SE-trending dextral strike-slip fault. This process might explain the wavy projection of the OSF.

5.2.3. Reconstruction at 2 Ma

When the collisional orogen continued to migrate from the NE to SW direction, the crust has lost its compressional support and become an area of crustal stretching (Teng, 1996). The top of the folded Unit Db was eroded to form the BU surface. The southwestwardly shallowing of BU surface toward Taiwan implies that the extensional regime has propagated from NE to SW offshore northern Taiwan (Fig. 8d). Because of a lack of Pliocene strata above the BU surface and the initiation of magmatic activities in northern Taiwan is suggested to be around
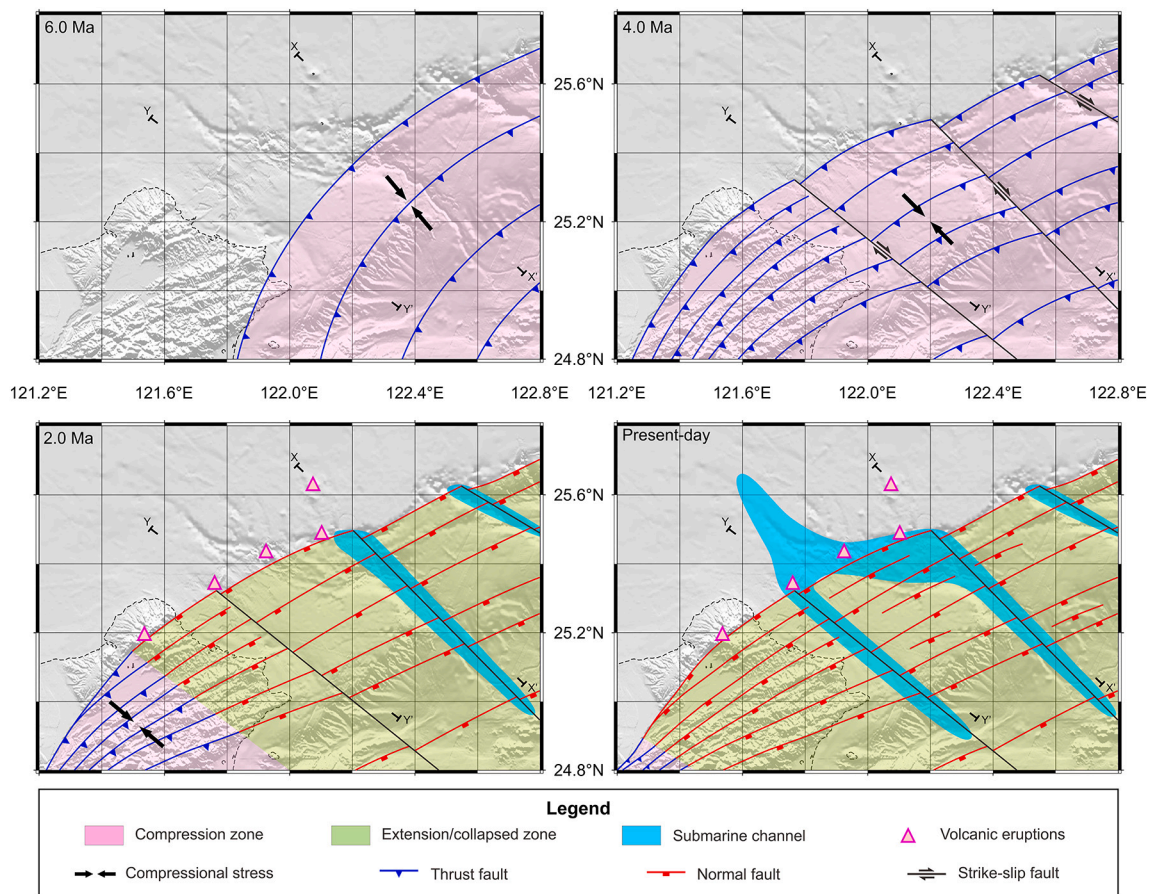
Fig. 9. Cartoons showing the geodynamic evolution in the offshore area of northern Taiwan. The Eurasia plate is fixed. Before ~6 Ma, offshore northern Taiwan was a rifted Eurasian continental margin. At ~6.0 Ma, the uplift of northern offshore Taiwan was due to the collision of the northern Luzon arc of the Philippine Sea plate with the continental margin. The northwesternmost thrust fault located roughly near the present-day Offshore Shanjiao Fault. A series of NW-SE-trending transpressional faults were formed due to the oblique collision at about 4.0 Ma. When the northern part of the mountain belt became an extensional setting, the NE-SW-trending thrust faults were reactivated as normal faults. Subsequently, the magma may have extruded along normal fault systems to form submarine volcanoes and volcanic islets since 2.5 Ma. The NW-SE-trending strike-slip faults also facilitated the development of the submarine channels. The Offshore Shanjiao Fault is the westernmost boundary of the crustal extensional regime in response to the opening of the southern Okinawa Trough since 2 Ma. The normal fault system continues its activity in the collapsed zone until the present-day. Cross-sections of XX' and YY' are shown in Fig. 10.

2.6–2.8 Ma (Wang et al., 2004), we suggest that the thrust belts offshore northern Taiwan started to collapse during the late Pliocene - early Pleistocene. The pre-existing NE-SW-trending thrust faults became tilted block faulting in the collapsed zone, forming a series of half-grabens. These normal faults probably also provide conduits for magma extrusion since the early Pleistocene (Wang et al., 2004), especially along the OSF. The NW-SE-trending dextral strike-slip faults could become transtensional zones, facilitating the development of the submarine canyons. The offshore area of northern Taiwan started to collapse probably at the same time when the southern Okinawa Trough back-arc basin started to open. Both two tectonic events could be closely related to the change of the westernmost Philippine Sea plate convergence from collision to subduction at ~2 Ma.

5.2.4. Present-day configuration

Due to both post-collisional subsidence and rifting of the southern Okinawa Trough, the extensional regime continues to propagate to present-day northern Taiwan. The extensional stress formed the Taipei Basin at around 0.8 Ma (Teng et al., 2001). Thick sediments of Unit F on both the shelf basin and the collapsed zone indicates that the sediments have accumulated rapidly (Fig. 7c-d). In the collapsed zone, the extensional regime not only enhances the NE-SW tilted block faulting but also creates new NE-SW-trending normal faults. In the shelf basin, several active faults occur near the OSF (SP 150–350, Fig. 5a), which indicates

that the active rifting not only exists in the back-arc basin of the southern Okinawa Trough but also in its northern continental margin.

6. Conclusions

We integrate drilled borehole stratigraphy and seismic data collected in the offshore area of northern Taiwan to understand the tectonic evolution off NE Taiwan in the late Cenozoic. Our reflection seismic data reveals that the Offshore Shanjiao Fault (OSF), a large offset and NE-SW-trending normal fault, is the offshore continuation of the onshore Shanjiao Fault. The OSF delimits the flat-lying shelf basin in the west and the blocked faulted collapsed zone in the east. The OSF was the thrust front during the collisional stage and has become a normal fault after the change of the stress regime from compression to extension at ~2 Ma.

The Oligocene-Miocene strata can be observed in both the shelf basin and the collapsed zone, indicating that the East China shelf basin extended to the east of the present collapsed zone prior to the collision. In other words, the collapsed zone was a part of the East China shelf basin before 6 Ma. In the collapsed zone, many large-offsets, NE-SW-trending normal faults could be reactivated from pre-existing thrust faults. However, these NE-SW-trending faults could not connect from onshore to offshore easily because their structures have been affected by the existence of NW-SE-trending strike-slip faults. The NW-SE-trending
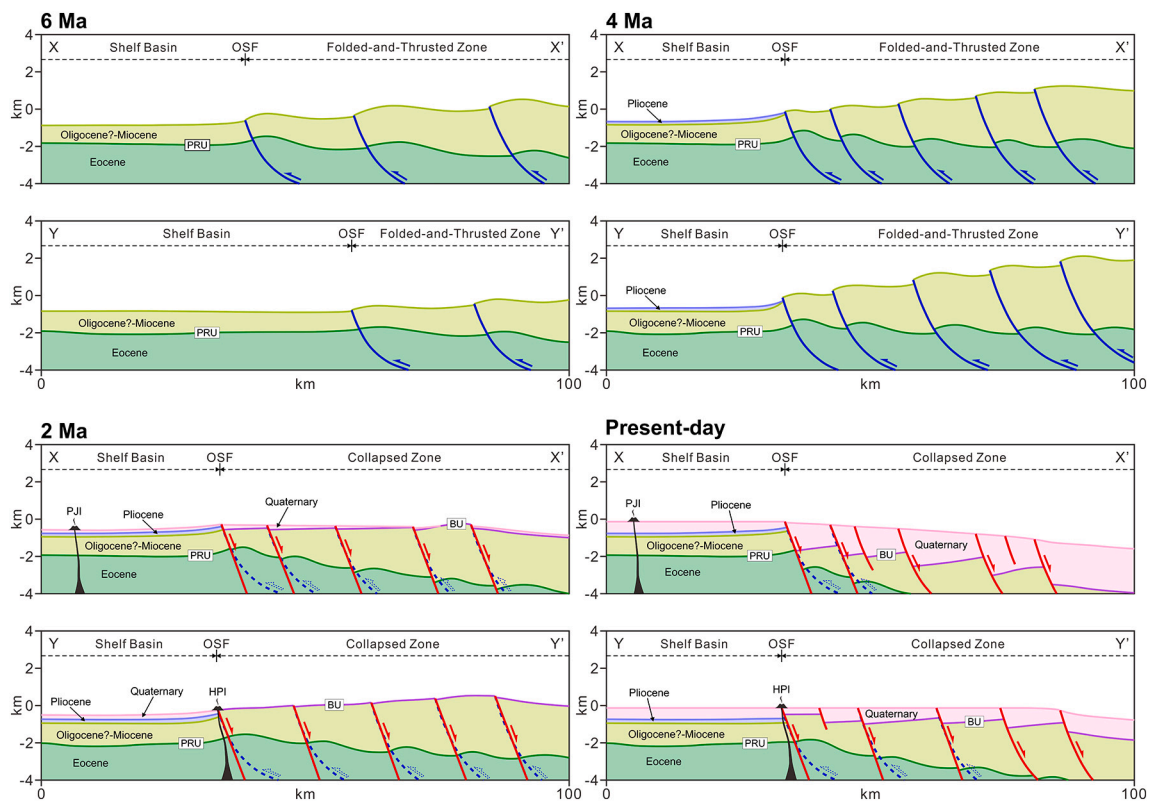
Fig. 10. Cross sections of the tectono-sedimentary evolution in the offshore area of northern Taiwan. OSF: Offshore Shanjiao Fault, PRU: Post-Rift Unconformity, BU: Basal Unconformity, HPI: Huaping islet, PJI: Pengjia islet, curved blue lines: Thrust faults, Curved red lines: Normal faults. See locations of cross sections XX' and YY'. (For interpretation of the references to colour in this figure legend, the reader is referred to the web version of this article.)

strike-slip faults probably favor the development of the submarine channels across the continental margin.

The Oligocene-Miocene strata in the collapsed zone were folded and their tops were eroded and formed the angular basal unconformity (BU). The SW-shallowing of the BU surface and thinning of the Quaternary strata toward the Taiwan island indicate that the extensional regime has propagated from NE to SW off northern Taiwan since the early Quaternary. We suggest that the offshore area of the northern Taiwan orogen started to collapse in the early Pleistocene, probably coeval with the early back-arc extension of the southern Okinawa Trough.

Credit author statement

- Quang-Minh Nguyen: Conceptualization, Data curation, Formal analysis, Writing - Original Draft, Writing- Review & Editing.
- Shu-Kun Hsu: Supervision, Funding acquisition, Conceptualization, Writing - Original Draft, Writing- Review & Editing.
- Andrew Tien-Shun Lin: Formal analysis, Validation, Editing.
- Chih-Cheng Yang: Formal analysis, Editing.

Declaration of Competing Interest

The authors declare that they have no known competing financial interests or personal relationships that could have appeared to influence the work reported in this paper.

Acknowledgments

References

Blackie, A.M., Carlson, C.T., Reed, K.J., Perez-Roca, E., 1975. Offshore Taiwan - East China Sea Block-C, Laohu-1x Wildcat (YCL-1) Completion Report. Gulf Oil Company of China, Taiwan Branch, 35 pp.

Chang, J.-H., Yang, Y.-C., Hsu, H.-H., Su, C.-C., Liu, C.-S., Chiu, S.-D., Ma, Y.-F., Li, Y.-W., Lin, Y.-C., Shen, J.-S., 2017. Seismic stratigraphic features of the Late Miocene-Present unconformities and related seismic units, northern offshore Taiwan. In: Aiello, G. (Ed.), Seismic and Sequence Stratigraphy and Integrated Stratigraphy - New Insights and Contributions. Intech Open. https://doi.org/10.5772/intechopen.70819.

Chang, J.-H., Yang, E.Y.-C., Hsu, H.-H., Chen, T.-T., Liu, C.-S., Chiu, S.-D., 2021. Igneous activity and structural development of the Mianhua Terrace, Offshore North Taiwan. Minerals 11 (3), 303. https://doi.org/10.3390/min11030303.

Hall, R., 2002. Cenozoic geological and plate tectonic evolution of SE Asia and the SW Pacific: computer-based reconstructions, model and animations. J. Asian Earth Sci. 20, 353–431.

Hsiao, L.-Y., Lin, K.-A., Huang, S.T., Teng, L.S., 1998. Structural characteristics of the southern Taiwan-Sinzi folded zone. Petrol. Geol. Taiwan 32, 133–153.

Hsu, S.-K., Sibuet, J.-C., 1995. Is Taiwan the result of arc-continent or arc-arc collision? Earth Planet. Sci. Lett. 136, 315–324.

Hsu, S.-K., Sibuet, J.-C., Monti, S., Shyu, C.-T., Liu, C.-S., 1996. Transition between the Okinawa Trough back-arc extension and the Taiwan collision: New Insights on the Southernmost Ryukyu Subduction Zone. Mar. Geophys. Res. 18, 163–187.

Hsu, S.-K., Sibuet, J.-C., Shyu, C.-T., 2001. Magnetic inversion in the East China Sea and Okinawa Trough: Tectonic implications. Tectonophysics 333, 111–122.

Hsu, S.-K., Yeh, Y.-C., Sibuet, J.-C., Doo, W.-B., Tsai, C.-H., 2013. A mega-splay fault system and tsunami hazard in the southern Ryukyu subduction zone, Earth Planet. Sci. Lett. 362, 99–107.

Kimura, M., 1985. Back-arc rifting in the Okinawa Trough. Mar. Pet. Geol. 2, 222–240.

Kong, F., Lawver, L.A., Lee, T.-Y., 2000. Evolution of the southern Taiwan-Sinzi Folded Zone and opening of the southern Okinawa Trough. J. Asia Earth Sci. 18, 325–341.

Lee, Y.-H., Byrne, T., Wang, W.-H., Lo, W., Rau, R.-J., Lu, H.-Y., 2015. Simultaneous mountain building in the Taiwan orogenic belt. Geology 43 (5), 451–454.

Letouzey, J., Kimura, M., 1985. Okinawa Trough genesis: Structure and evolution of a back-arc basin developed in a continent. Mar. Pet. Geol. 2, 111–130.

Lin, A.T., Liu, C.-S., Lin, C.-C., Schnurle, P., Chen, G.-Y., Liao, W.-Z., Teng, L.S., Chuang, H.-R., Wu, M.-S., 2008. Tectonic features associated with the overriding of

an accretionary wedge on top of a rifted continental margin: An example from Taiwan. Mar. Geol. 255, 186–203.

Malavieille, J., Lallemand, S.E., Dominguez, S., Deschamps, A., Lu, C.-Y., Liu, C.-S., Schnuerle, P., 2002. Geology of the arc-continent collision in Taiwan: Marine observations and geodynamic model. Geol. Soc. Am. Spec. Issue 358, 187–211.

Mitchum, R.M., Vail, P.R., Thompson, S., 1997. Seismic stratigraphy and global changes of sea level, Part 2: The depositional sequence as a basic unit for stratigraphic analysis. In: Payton, C.E. (Ed.), Seismic Stratigraphy-Applications to Hydrocarbon Exploration. American Association of Petroleum Geologist Memoir 26, Tulsa, Oklahoma, U.S.A, pp. 53–62.

Seno, T., Stein, S., Gripp, A.E., 1993. A model for the motion of the Philippine Sea Plate consistent with NUVEL-1 and geologic data. J. Geophys. Res. 98, 17941–17948.

Sibuet, J.-C., Hsu, S.-K., 2004. How was Taiwan created? Tectonophysics 379, 159–181.

Sibuet, J.-C., Hsu, S.-K., Shyu, C.-T., Liu, C.-S., 1995. Structural and kinematic evolution of the Okinawa Trough back-arc basin. In: Taylor, B. (Ed.), Back-arc Basins: Tectonics and Magmatism. Plenum, New York, pp. 343–378.

Sibuet, J.-C., Deffontaines, B., Hsu, S.-K., Thareau, N., Le Formal, J.-P., Liu, C.-S., the ACT Party, 1998. Okinawa Trough back-arc basin: Early tectonic and magnetic evolution. J. Geophys. Res. 103, 30245–30267.

Sibuet, J.-C., Hsu, S.-K., Le Pichon, X., Le Formal, J.P., Reed, D., Moore, G., Liu, C.-S., 2002. East Asia plate tectonics since 15 Ma: Constraints from the Taiwan region. Tectonophysics 344, 103–134.

Song, G.-S., Ma, C.-P., Yu, H.-S., 2000. Fault-controlled genesis of the Chilung Sea Valley (northern Taiwan) revealed by topographic lineaments. Mar. Geol. 169, 305–325.

Sun, S.-C., 1985. The Cenozoic tectonic evolution of offshore Taiwan. Energy 10 (3/4), 421–432.

Suppe, J., 1984. Kinematic of arc-continent collision, flipping of subduction, and back-arc spreading near Taiwan. Mem. Geol. Soc. China 6, 21–33.

Teng, L.S., 1990. Geotectonic evolution of late Cenozoic arc-continent collision in Taiwan. Tectonophysics 183, 67–76.

Teng, L.S., 1996. Extensional collapse of the northern Taiwan mountain belt. Geology 24, 949–952.

Teng, L.S., Lin, A.T., 2004. Cenozoic tectonics of the China continental margin: insights from Taiwan. Geol. Soc. Lond., Spec. Publ. 226, 313–332.

Teng, L.S., Lee, C.-T., Tsai, Y.-B., Hsiao, L.-Y., 2000. Slab breakoff as a mechanism for flipping of subduction polarity in Taiwan. Geology 28, 155–158.

Teng, L.S., Lee, C.-T., Peng, C.-H., Chen, W.-F., Chu, C.-J., 2001. Origin and geological evolution of the Taipei basin, northern Taiwan. West. Pacific Earth Sci. 1 (2), 115–142.

Tsai, C.-H., Huang, C.-L., Hsu, S.-K., Doo, W.-B., Lin, S.-S., Wang, S.-Y., Lin, J.-Y., Liang, C.-W., 2018. Active normal faults and submarine landsides in the Keelung Shelf off NE Taiwan. Terr. Atmos. Ocean. Sci. 29 (1), 31–38.

Tsai, C.-H., Hsu, S.-K., Chen, S.-C., Wang, S.-Y., Lin, L.-K., Huang, P.-C., Chen, K.-T., Lin, S.-S., Liang, C.-W., Cho, Y.Y., 2021. Active tectonics and volcanism in the southernmost Okinawa Trough back-arc basin derived from deep-towed sonar surveys. Tectonophysics 817, 229047.

Twiss, R.J., Moores, E.M., 1992. Structural Geology. W.H. Freeman and Company, New York, p. 532p.

Vail, P.R., Mitchum, R.M., 1977. Seismic stratigraphy and global changes of sea level, Part 1: overview. In: Payton, C.E. (Ed.), Seismic Stratigraphy-Applications to Hydrocarbon Exploration. American Association of Petroleum Geologist U.S.A, pp. 51–52.

Wang, K.-L., Chung, S.-L., O'Reilly, S.Y., Sun, S.-S., Shinjo, R., Chen, C.-H., 2004. Geochemical constraints for the genesis of post-collisional magmatism and the geodynamic evolution of the northern Taiwan region. J. Petrol. 45 (5), 975–1011.

Wang, B., Doust, H., Liu, J., 2019. Geology and petroleum systems of the East China Sea Basin. Energies 12, 4088. https://doi.org/10.3390/en12214088.

Wessel, P., Luis, J.F., Uieda, L., Scharroo, R., Wobbe, F., Smith, W.H.F., Tian, D., 2019. The Generic Mapping Tools version 6. Geochem. Geophys. Geosyst. 20, 5556–5564.

Yang, C.-C., Yu, M.-R., Su, D.-F., 1985. Subsurface Geology Well Report of YAC-1. Geology Department, Offshore Exploration Division, Chinese Petroleum Corporation, p. 40.

Yu, H.-S., 2005. Nature and distribution of the deformation front in the Luzon Arc-Chinese continental margin collision zone at Taiwan. Mar. Geophys. Res. 25, 109–122.

Yu, S.-B., Chen, H.Y., Kuo, L.-C., 1997. Velocity field of GPS stations in the Taiwan area. Tectonophysics 274, 41–59.

Zhou, Z., Zhao, J., Yin, P., 1989. Characteristics and tectonic evolution of the East China Sea. Sediment. Basins World 1, 165–179.